The Company of Biologists

RESEARCH ARTICLE

Mammals repel mosquitoes with their tails

Marguerite E. Matherne[1], Kasey Cockerill[1], Yiyang Zhou[1], Mihir Bellamkonda[1] and David L. Hu[1,2,*]

ABSTRACT

The swinging of a mammal's tail has long been thought to deter biting insects, which, in cows, can drain up to 0.3 liters of blood per day. How effective is a mammal's tail at repelling insects? In this combined experimental and theoretical study, we filmed horses, zebras, elephants, giraffes and dogs swinging their tails. The tail swings at triple the frequency of a gravity-driven pendulum, and requires 27 times more power input. Tails can also be used like a whip to directly strike at insects. This whip-like effect requires substantial torques from the base of the tail on the order of 10^1–10^2 N m, comparable to the torque of a sedan, but still within the physical limits of the mammal. Based on our findings, we designed and built a mammal tail simulator to simulate the swinging of the tail. The simulator generates mild breezes of 1 m s^{-1}, comparable to a mosquito's flight speed, and sufficient to deter up to 50% of mosquitoes from landing. This study may help us determine new mosquito-repelling strategies that do not depend on chemicals.

KEY WORDS: Mammal tail, Defense, Mosquito

INTRODUCTION

Mammals have a rich suite of behaviors to repel insects from their bodies, including tail-swatting, head-shaking, foot-stomping and muscle-twitching (Mooring et al., 2007). Elephants will even pick up fallen tree branches with their trunks and use them to swat at flies on their backs and sides (Moore, 2002). In this study, we were interested in the role tails play in repelling insects. Tails in mammals serve many purposes, including defense, balance, communication and locomotion (Hickman, 1979). Many investigators have assumed that the tail is used to defend against insects (Mooring et al., 2007; Hickman, 1979; Samuel et al., 2001; Lefebvre et al., 2007; Siegfried, 1990), as shown in Fig. 1A. The best evidence that tails are used to defend against biting insects is that the frequency of tail swishes increases with the number of insects present (Mooring et al., 2007). In the present study, we investigate how mammal tails defend against insects.

Biting insects, such as mosquitoes (Fig. 1B), black flies and horse flies, pose a significant threat to both domestic and wild mammals. They can cause irritation, loss of blood, loss of resting and feeding time, disease infection and death (Samuel et al., 2001; Mooring et al., 2007). Up to 1000 flies per hour have been observed to land on horses (Foil and Foil, 1988), and cows can lose 300 ml of blood per day owing to horse flies (Tashiro and Schwardt, 1953). Stable flies alone are estimated to cost the US cattle industry $2.2 billion

per year through reduced milk production and reduced mass gain (Taylor et al., 2012). Bot and warble flies deposit their eggs on the hairs of mammals and cause myiasis, the larval infestation of live vertebrates that eat the host's tissue. Bot flies are highly host-specific, ranging from mice to elephants (Cowell et al., 2006), and can cause a reduction of mass gain of 20 to 27 kg per year in cattle (Hart, 1990). Clearly, any behavior that prevents such flies from landing and biting will be beneficial to the host animal and be selected for in subsequent generations.

Defensive behavior is a mammal's main repellant of insects (Moore, 2002) and it has been long studied (Harvey and Launchbaugh, 1982; Keiper and Berger, 1982; Waage and Nondo, 1982; Edman and Scott, 1987; Warnes and Finlayson, 1987; Toupin et al., 1996; Horváth et al., 2010). In fact, when biting insects are choosing a host, the primary selection factor is the type of defensive behavior exhibited (Moore, 2002). Calves that defend themselves more are attacked by fewer stable flies than those who are less active (Warnes and Finlayson, 1987). Ungulates stand in large groups to reduce the number of insect bites per individual by spreading the attacks among the crowd (Mooring and Hart, 1992). Horses often stand next to one another head-to-tail or head-to-shoulder and swish their tails to protect the head and hindquarters of their neighbors (Lefebvre et al., 2007). All of these defensive actions require the expenditure of energy. Howler monkeys use up to 24% of their basal metabolism to slap their forearms to remove or deter insects (Dudley and Milton, 1990).

Humans have designed a number of insect-repelling devices that mimic the mammal tail. Fly whisks, as shown in Fig. 1C,D, were designed to repel flies and other insects. They were made of the tail hair of yaks, oxen or horses (Beer, 2003; Williams, 2006). In use for thousands of years (Riegel, 1979), they eventually became a symbol of royalty (Beer, 2003), or authority and power (Riegel, 1979). In religions such as Buddhism or Jainism (Beer, 2003; Williams, 2006), fly whisks ward off insects without killing them. The fly whisk even led Algeria into war in 1827, when the Dey of Algiers angrily struck the French ambassador three times with his fly whisk because France refused to pay their debts. France responded by blockading the port of Algiers and led to the French rule of Algeria that lasted 132 years (Rogan, 2012). Today, mammal tails continue to inspire the design of insect-repelling devices. One example is the ShooAway™, a device advertised 'to effortlessly and efficiently keep flies off your food' (www.shooawayusa.com). The device spins two blades with shiny, 'holographmatic disks' on the end of the blades. In this study, we compare the effectiveness of this device with that of a mammal tail.

We first provide our detailed materials and methods. We then present the kinematics and air flows generated by a swishing tail, and explain the dynamics that control a tail when it is swatting at an insect. We conclude with a discussion of the repercussions of our study.

MATERIALS AND METHODS
Frequency of tail swishes

The tail swishing behaviors of zebras (*Equus quagga*), giraffes (*Giraffa camelopardalis*) and African elephants (*Loxodonta*

[1]School of Mechanical Engineering, Georgia Institute of Technology, Atlanta, GA 30332, USA. [2]School of Biology, Georgia Institute of Technology, Atlanta, GA 30332, USA.

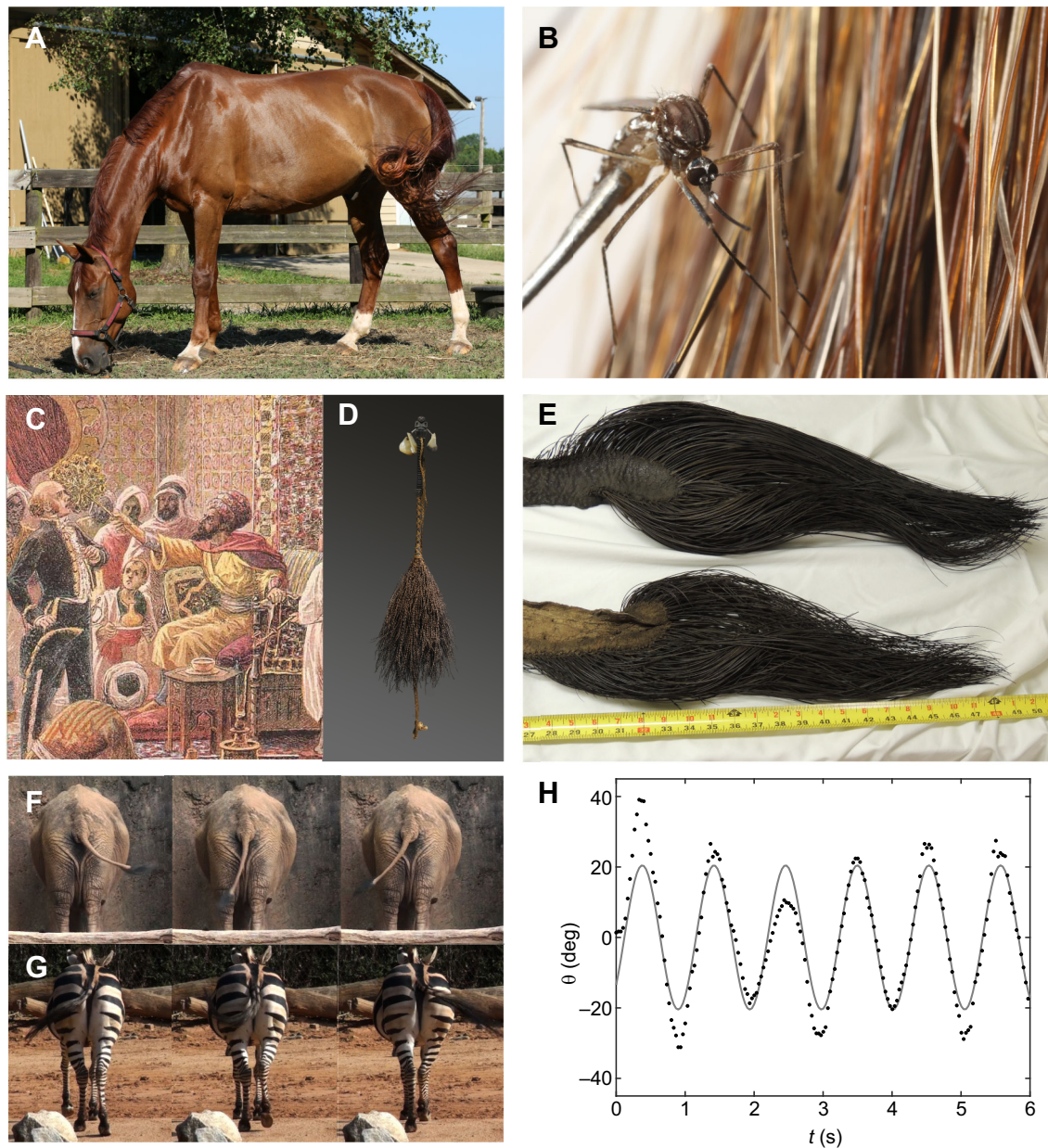*Author for correspondence (hu@me.gatech.edu)

D.L.H., 0000-0002-0017-7303

Fig. 1. Tail swishing by mammals. (A) A horse swishes its tail to ward off attacking insects. Photo by Candler Hobbes. (B) A mosquito interacts with the hairs of an imitation horse tail. Photo by Candler Hobbes. (C) Depiction of the Fly Whisk Incident of 1827 in Algiers. By Anonymous [public domain], via Wikimedia Commons. (D) A late 18th to early 19th century fly whisk from the Austral Islands (Polynesia). By Demarque Denis (own work) [CC BY-SA 4.0], via Wikimedia Commons. (E) Elephant tail showing where the bone and skin part of the tail ends and the hairy part begins. Time-lapse image sequences of (F) elephant and (G) zebra. Elephant images are separated by 0.33 s and zebra images are separated by 0.17 s. (H) Time course of the angle of a zebra's tail. Solid points are experimental data and the solid line is a sinusoidal fit given in Table S2.

africana) were filmed at Zoo Atlanta (Atlanta, GA, USA); horses (*Equus caballus*) were filmed at Falcon Ridge Stables in Woodstock, GA; and dogs (*Canis lupus familiaris*) were filmed at a local dog park between the months of July and November. This study was approved by the Office of Research Integrity Assurance and conducted in accordance with all protocols filed under the Georgia Institute of Technology Institutional Animal Care and Use Committee. Tracker Video Analysis and Modeling Tool software (https://physlets.org/tracker/) was used to track the tail movements. MATLAB was used to calculate fits of the data using the least-squares method.

The number of periods to measure the frequency and amplitude of the swish were: elephant, 9; giraffe, 7; zebra, 7; horse, 11; and dogs,

8, 9, 5, 13, 17, 9, 16 and 9. The mass of the zoo animals, horse, Greyhound, Irish Setter and mixed breed dogs is the mass of the individual animal, measured in the past year by the animal's caretakers, while the mass of the other dogs is the average mass of that breed and gender. The body mass, tail length, tail swish frequency, tip speed and amplitude for each animal are shown in Fig. 2 and given in Table S1, and the sinusoidal fits for each animal's tail swing is given in Table S2.

Mosquito experiments

We obtained mosquitoes (*Aedes aegypti*) from the Centers for Disease Control and Prevention in Atlanta, GA, USA. The mammal

tail simulator with the fan attachment consisted of a black, 18 cm long and 1.7 cm wide plastic blade attached to a DC-powered motor. The fan was attached to a plastic board and placed face down on a 30 cm tall, 19.5 cm inner diameter clear acrylic cylinder with open top face, as shown in Fig. 3A.

The oscillating, single blade attachment setup used the same cylinder and top board with a 12 V, 7.5 deg step stepper motor (SparkFun Electronics ROB-10551, Niwot, CO, USA) controlled by an Arduino Uno microcontroller board. A single, 7.9 cm long, 1.7 cm wide blade made of black construction paper was used to oscillate over 180 deg. A plastic sheet was used to divide the cylinder in half and contain the mosquitoes in the area over which the blade oscillated, as shown in Fig. 3B.

For the ShooAway™ experiments, a cylinder made from clear plastic sheets was glued to a cardboard square, and the ShooAway™ was inverted so that the blades spun in the cylinder just below the cardboard square, as shown in Fig. 3C.

The following procedures were used for the steady-state fan, the oscillating fan and the ShooAway™ experiments. For each trial, 10 mosquitoes were placed inside the container using an aspirator with a HEPA filter (BioQuip 1135Y, Rancho Dominguez, CA, USA). At the beginning of each trial, the cage was manually shaken until all mosquitoes had taken flight. The fan was turned on immediately after all mosquitoes took flight. The fan was run for a time interval of 2 min, chosen because the mosquitoes all landed well within 2 min, and once they land they tend not to move. At the end of the trial, the fan was turned off and the number of mosquitoes on the ceiling of the setup (including on or behind the fan blade itself) was recorded.

The flight paths of mosquitoes were tracked with the fan either off or moving at a tip speed of 380 cm s^{-1} (6 Hz) using Tracker Video Analysis and Modeling Tool software as shown in Fig. 4.

Modeling the double pendulum

To understand the dynamics behind tail swishing, we modeled the tail as a double pendulum, a diagram of which is shown in Fig. 5A. The top hinge corresponds to the point where the caudal vertebrae begin to extend away from the body (point 1), the hinge connecting the two segments corresponds to the point where the bone and skin part of the tail end (point 2), and the bottom point corresponds to the end of the hair (point 3). The double pendulum is modeled as having a center of mass at the midpoint of each pendulum. The equations of motion for this pendulum can be derived using the Lagrangian equation:

$$\frac{\partial}{\partial t}\left(\frac{\partial L}{\partial \dot{\theta}_i}\right) - \frac{\partial L}{\partial \theta_i} = \tau_i, \qquad (1)$$

where $L=T-V$, T is the kinetic energy of the system, V is the potential energy of the system, the subscript i denotes the pendulum ($i=1$ or 2) as shown in Fig. 5A, t is time, θ_i is the angle of pendulum i from the vertical as shown in Fig. 5A, $\dot{\theta}_i$ is the time derivative of θ_i and τ_i is

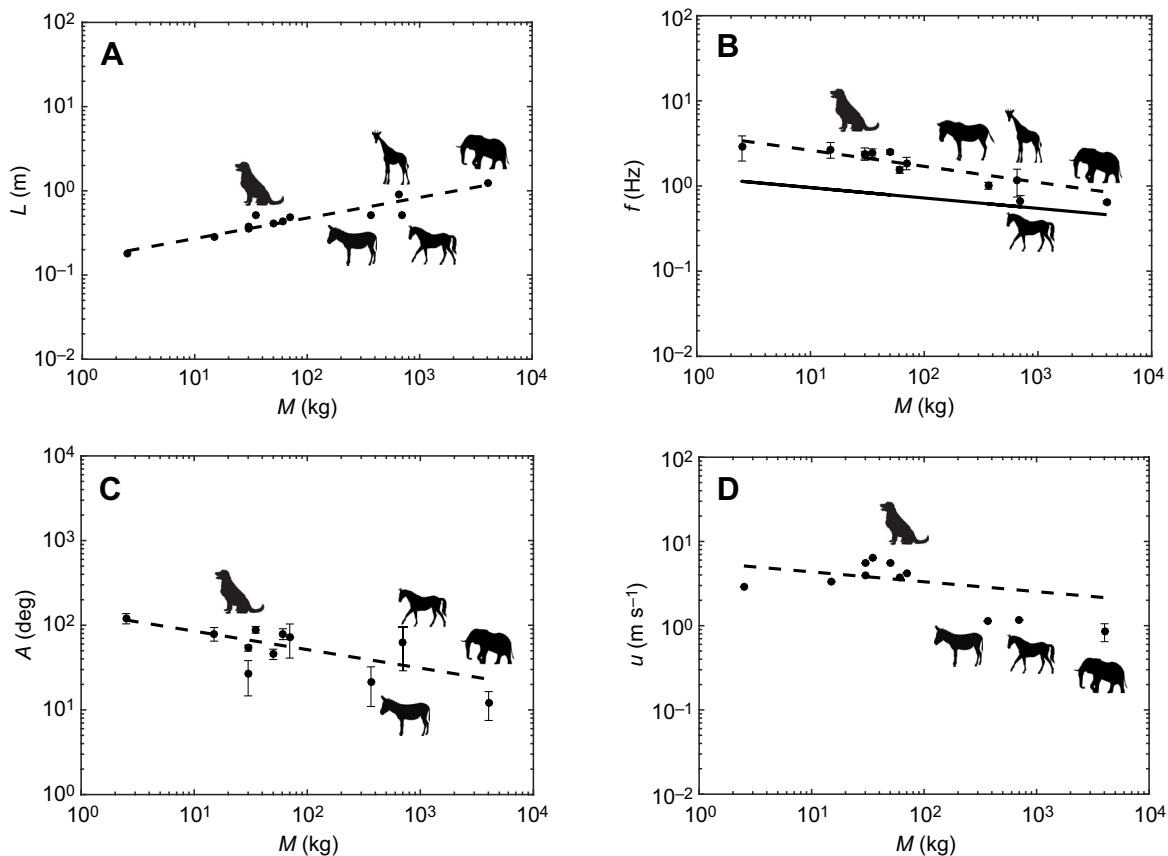Fig. 2. The kinematics of tail-swishing. Relationships between body mass and (A) tail length L, (B) tail frequency f, (C) tail amplitude A and (D) tail tip speed u. Dashed line is fit of the data and error bars are the standard deviation of each measurement. In B, solid line is the natural frequency of the tail. The number of periods, N, used for calculating the frequency, amplitude and tip speed for each animal are given in Table S1. The data in A are only one measurement for each animal, as described in the Materials and Methods.
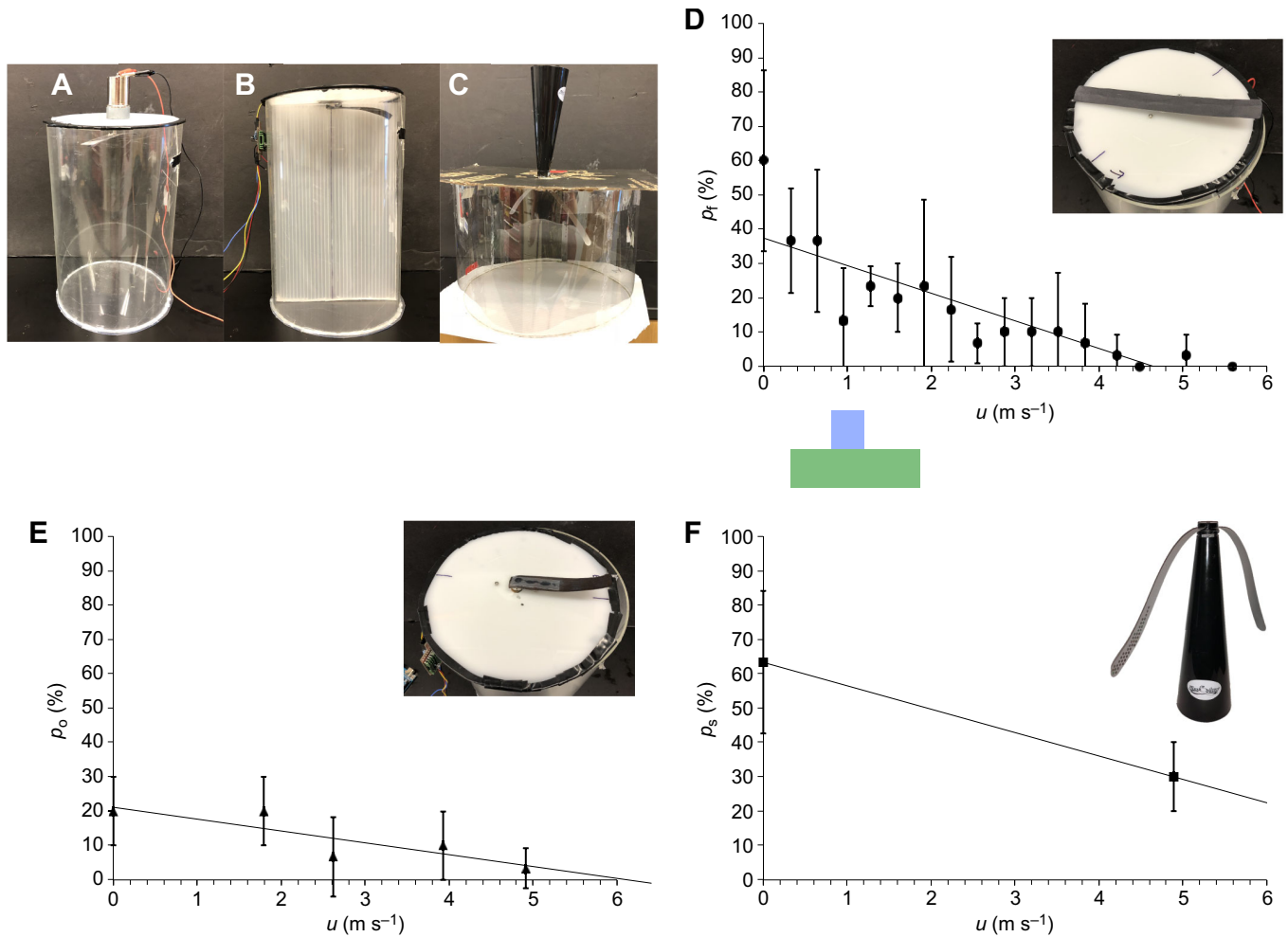
Fig. 3. Effects of tail motion on mosquitoes. Schematic of the mammal tail simulator with (A) fan attachment, (B) oscillating attachment and (C) the inverted ShooAway™. (D–F) Relationship between tip speed u and percentage p of mosquitoes that land on the top of the mammal tail simulator for (D) the fan attachment, (E) the oscillating attachment and (F) the ShooAway™ at the average tip speed correlating to its varying frequency. The insets show the simulator attachment corresponding to the data. The blue rectangle in D represents the measured range for mammal tail tip speeds for the elephant, zebra and horse. Mosquito flight speed is represented by the green rectangle. The solid lines are the linear fit for the data.

the torque input into the top of pendulum i. This leads to the equations of motion (Greenwood, 2003):

$$\frac{m_1 L_1^2}{12}\ddot{\theta}_1 + \left(\frac{m_1 L_1^2}{4} + m_2 L_1^2\right)\ddot{\theta}_1 + m_2 L_1 L_2 \ddot{\theta}_2 \cos(\theta_2 - \theta_1)$$

$$+ m_2 L_1 L_2 \dot{\theta}_1 \dot{\theta}_2 \sin(\theta_1 - \theta_2) + \left(\frac{1}{2}m_1 + m_2\right)gL_1 \sin\theta_1 = \tau_1,$$

$$(2)$$

$$\frac{m_2 L_2^2}{12}\ddot{\theta}_2 + m_2 L_2^2 \ddot{\theta}_2 + m_2 L_1 L_2 \ddot{\theta}_1 \cos(\theta_2 - \theta_1)$$

$$+ m_2 L_1 L_2 \dot{\theta}_1 \dot{\theta}_2 \sin(\theta_1 - \theta_2) + m_2 g L_2 \sin\theta_2 = 0,$$

$$(3)$$

where $\ddot{\theta}_i$ is the second time derivative of θ_i, m_i and L_i are the mass and length of pendulum i, respectively, and g is the gravitational acceleration. There is a torque input into the system only at point 1, with no input torque at point 2. The initial conditions to the system are the pendulum at rest with $\theta_1=\theta_2=0$.

RESULTS

Tail swishing

Frequency of tail swishes

We filmed five species of mammals at a series of locations including Zoo Atlanta, a stable and a dog park. In all, we filmed an African elephant, a giraffe, a zebra, a horse and eight dogs. All of the animals observed performed swings with their tail as well as swats, where they struck their own body. We filmed between the months of July and November, and were harassed by many insects while filming, so we are assured that there were biting insects present. The insects were too small to see in the videos, so we assumed that swats occurred because the animal felt an insect landing on it.

Movie 1 shows representative videos of the zebra, horse, giraffe and elephant swishing their tails. We tracked the end of the tail, defined as the end of the last bone in the tail as can be seen in Fig. 1E, using 5–17 periods for each animal. The average tail lengths of the zebra, giraffe and elephant were obtained from the literature (Nowak, 1999), whereas the tail lengths of the horse and the eight dogs were measured.
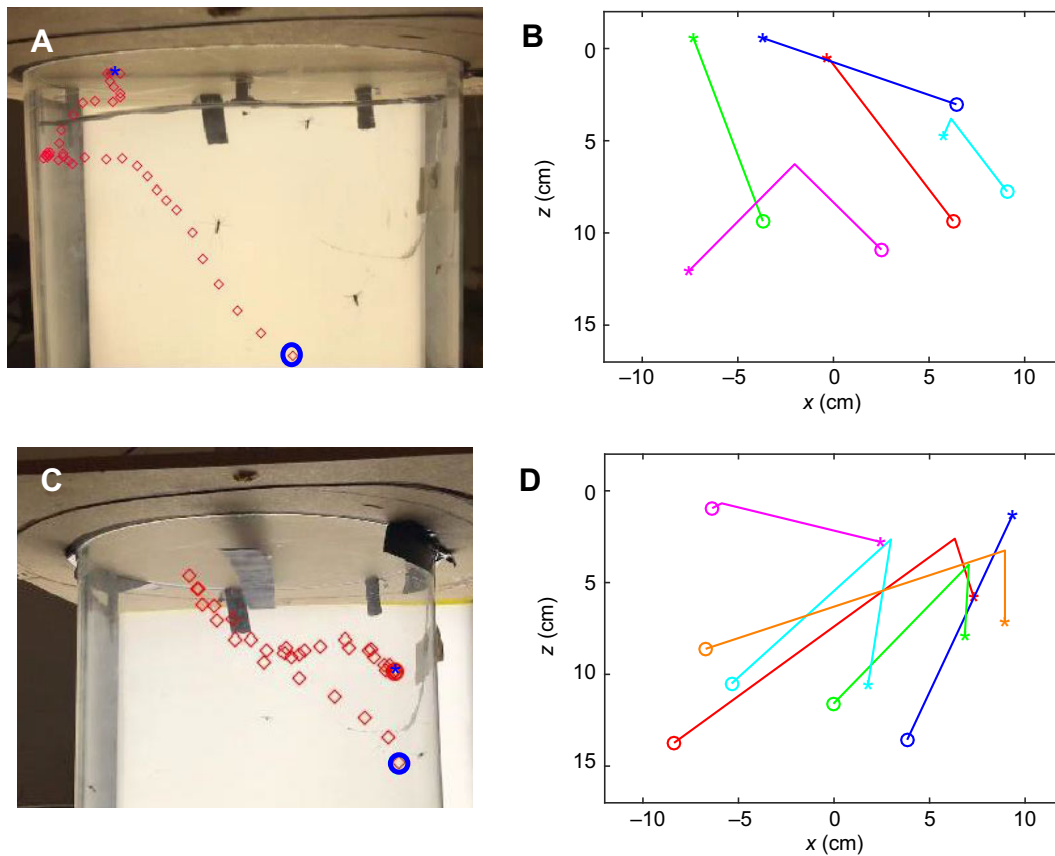
Fig. 4. Mosquito tracks in the mammal tail simulator with the fan attachment. Examples of flight path of mosquitoes in the mammal tail simulator with the fan off (A,B) and the fan on (C,D). The red diamonds in A and C are the mosquitoes being tracked by Tracker Software. Mosquitoes begin at the points marked by circles, reach a maximum height and then eventually land at the points marked by the asterisks.

Fig. 1F,G shows a time lapse of the tail swish of an elephant and zebra, respectively, and Fig. 1H shows the time course of the angle θ_1 of the tail of a zebra, where $\theta_1=0$ is associated with the tail hanging vertically downward. Long, slender pendulums such as the tail usually follow simple harmonic motion, where the angle is prescribed by:

$$\theta(t) = A\sin(2\pi ft), \quad (4)$$

where A is the amplitude of the motion, f is the frequency in Hz and t is time. We applied Eqn 4 to all of the films of mammal tails to infer their amplitude and frequency. For example, such simple harmonic motion is a good fit ($R^2=0.84$) to the motion of the zebra tail, as shown in Fig. 1H. The data are shown by the black points and the theoretical fit is shown by the solid line. In this case, the theoretical fit is $\theta(t)=20\sin(6.0t)$, where θ is in degrees, t is in seconds and the coefficients are found using least-squares fitting.

The rotational velocity may be written as $\dot{\theta}\sim 2\pi Af$, and the maximum tail tip speed (u) is therefore:

$$u = 2\pi LAf, \quad (5)$$

where L is the length of the tail and A has been converted to radians. The zebra tail has a maximum tail tip speed of 1.1 m s^{-1}, frequency of 1.0 Hz and amplitude of 22 deg.

The experimental measurements for the length (m), frequency (Hz), amplitude (deg) and tip velocity (m s^{-1}) of the tail are given in Fig. 2. The values for each animal are given in Table S1. The dashed lines in these figures correspond to power law best fits using least-squares:

$$L = 0.15M^{0.24} \quad (R^2 = 0.85), \quad (6)$$

$$f = 4.0M^{-0.19} \quad (R^2 = 0.81), \quad (7)$$

$$A = 140M^{-0.22} \quad (R^2 = 0.56), \quad (8)$$

$$u = 5.7M^{-0.12} \quad (R^2 = 0.26), \quad (9)$$

where M is the mass of the animal in kg. Eqn 6 shows that larger mammals have relatively shorter tails. In other words, tail length is not isometric, where isometry indicates that body proportions are independent of body size and thus scale with mass to the power of 1/3 (McMahon, 1975).

Larger animals swish their tails less vigorously than smaller ones. Tail amplitude ranges from 12 deg in an elephant to 120 deg in a dog. Body size also leads to associated differences in tail swishing style. The tail swish of the giraffe, elephant and zebra are in plane, permitting the motion to be visualized from a single view behind the animal. The horse swishes its tail in a similar manner, but because it has such long hair the swish becomes three-dimensional, with the hairs wrapping around the animal's flanks at the end of the swing. Dog's tails are often raised above their
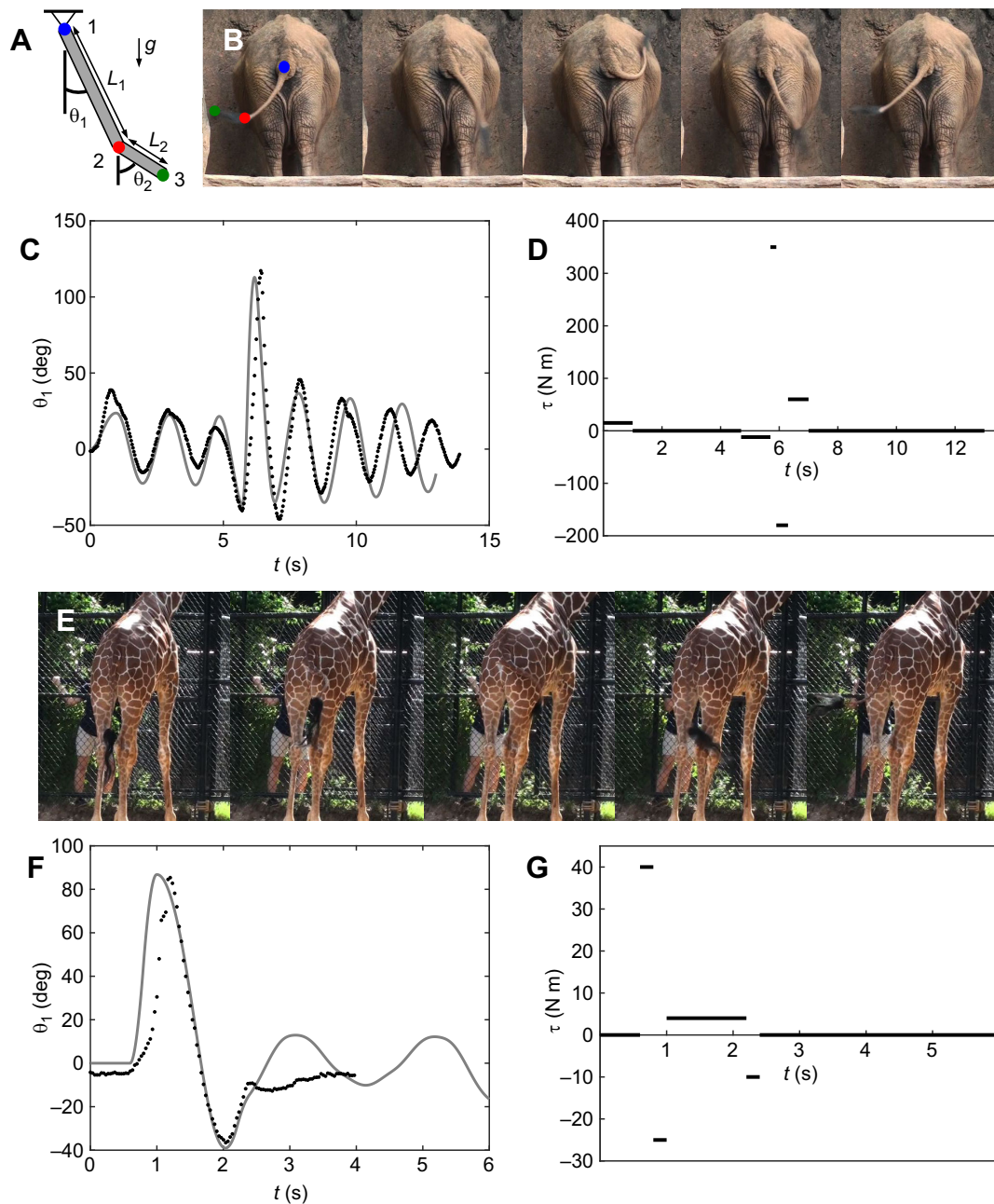
Fig. 5. Swatting by mammal tails. (A) Schematic of the tail, idealized as a double pendulum. θ_1 is the angle of the first link in the double pendulum, θ_2 is the angle of the second link, L_1 is the length of the first link, L_2 is the length of the second link and g is gravitational acceleration. 1, 2 and 3 denote the points of the tail we tracked. (B,E) Time-lapse image sequences of an elephant (B) and giraffe (E) swatting at an insect. Elephant images are separated by 0.23 s and giraffe images are separated by 0.33 s. (C,F) Time course of the tail angles θ_1 (deg) of the elephant (C) and giraffe (F). Solid line represents the predictions of the theoretical model. (D,G) Applied torque τ to the base of the tail of the elephant (D) and giraffe (G).

bodies instead of hanging down, and they swish in a plane. Therefore, the angle of the dog tail is measured relative to the tail pointing vertically upward.

We initially hypothesized that the animal should swish its tail at its natural frequency, the frequency of a gravity-driven pendulum:

$$f_n = \frac{1}{2\pi}\sqrt{\frac{g}{L}}, \qquad (10)$$

where f_n is in radians per second, g is the gravitational acceleration and L is the tail length. This is the frequency that conserves the most

energy for the animal because gravitational potential energy is transferred to kinetic energy in each swing. To minimize the energy consumed, most man-made devices such as grandfather clocks and metronomes swing at their natural frequency. Surprisingly, mammal tails do not.

By substituting Eqn 6 into Eqn 10, we write the natural frequency (Hz) in terms of body mass (kg):

$$f_n = 1.3M^{-0.12}. \qquad (11)$$

Fig. 2B shows the best fit for tail frequencies in a dashed line and their natural frequencies in a solid line. The two lines are nearly

parallel, as can be seen from the comparable exponents for these equations (−0.19 versus −0.12). This suggests that the physics of a gravity-driven pendulum can account for the trends according to body size. Most notable, however, is that the natural frequencies are 3.1 times lower than the observed tail frequency, which can be seen by comparing the pre-factors in Eqns 7 and 11. Why would mammals want to swing their tails three times faster than they would naturally swing by gravity?

The costs of choosing such a high frequency are made clear by considering energetics. An upper bound for the power required to swing the tails may be written as:

$$P = \frac{1}{2} mL\dot{\theta}^2 (2\pi f) = 4\pi^2 mLA^2 f^3, \qquad (12)$$

where m is the mass of the tail. This is an upper bound because we assume that the tail energy is dissipated on every swing. Because the tail frequency f is three times greater than the natural frequency, we conclude that the power use is $(P_{tail}/P_{grav}) = (f^3/f_n^3) = 27$ times greater. Why would mammals want to expend so much energy with their tails?

Our first consideration is that the tail acts to deflect mosquitoes by hitting them in mid-air. Solving this problem is similar to counting the number of raindrops striking one's head (Walker, 2007). The density ρ of mosquitoes per volume is assumed by considering a square lattice of mosquitoes near the ground, where $\rho = c/L$ and c is 80 mosquitoes per acre (Gillies, 1955). If we assume the mosquitoes are stationary objects in mid-air, how often does a swinging tail make contact? Consider the tail as a square prism with length L and width w. Using conservation of mass, we can write the rate of mosquitoes $\dot{m}$ being struck by the tail as:

$$\dot{m} = \int_{r=0}^{r=L} w\rho u \, dr = \int_{r=0}^{r=L} w\rho(2\pi Af) r \, dr = \pi w\rho AfL^2, \qquad (13)$$

where A is in radians. We consider a horse with a measured frequency of 0.66 Hz, amplitude of 63 deg, tail width of 0.18 m and full tail length, which includes both the bony and hairy parts of the tail, of 1.4 m. Eqn 13 shows that an insect is struck every 1.5 min by the tail, which does not seem very effective at repelling mosquitoes. How does the tail effectively repel insects?

To answer this question, we purchased a horse whip made of horse tail hairs and tried to strike free-flying mosquitoes with it in our laboratory. We filmed the process and were surprised to find that even near-misses with the horse tail caused a resting mosquito to take off. This led us to hypothesize that the tail generates airflow that repels mosquitoes. To test this hypothesis, we designed and built a mammal tail simulator that tests the effectiveness of our measured tail kinematics in repelling mosquitoes.

Mammal tail simulator
Because mammal tails come in a variety of diameters and shapes, especially in the hair tufts at the end, we performed experiments using a simplified tail, consisting of a rectangular blade with no hair tufts. We conducted tests with two types of attachments, a propeller-like fan (Fig. 3A and the inset of 3D) and a single blade attachment (Fig. 3B and the inset of 3E). The fan is rotated in steady-state, and the single-blade performs oscillatory motion. We discuss the results for each of these experiments in turn. We also report tests with a commercial device, the ShooAway™ (Fig. 3C and the inset of 3F), that is purported to repel insects by spinning two flexible arms. We observed that mosquitoes do not like to land on smooth, curved surfaces and that they generally prefer to fly up rather than down.

Thus, we used a clear acrylic cylinder to contain the mosquitoes during the experiment.

For the steady-state experiments, a DC motor spun a fan representing the tail, a black rectangular plastic blade with a length 1 cm less than the inner diameter of the cylinder. The fan was located at the top of the cylinder, facing down. The blade was black because most mammal tails are black, although we did not try other colors of the blade. The DC motor was affixed to a plastic board, which represents the body of the animal and also prevents the mosquitoes from escaping. The board was the uppermost surface in the experiment. This arrangement ensured that most of the mosquitoes would attempt to fly up past the fan and land on the board. A video of mosquitoes flying in the simulator with the fan attachment is given in Movie 2.

A mammal swishes its tail in a sinusoidal motion, like a pendulum, while our tail simulator rotates steadily. To ensure that the difference between the two motions does not impact the simulator's ability to repel mosquitoes, we repeated the experiments using a single blade driven by a stepper motor oscillating over 180 deg in a periodic motion, as can be seen in Fig. 3B. The same clear acrylic cylinder was used, with the addition of a wall made from a rigid plastic sheet dividing the cylinder in half. This divider wall ensured that the tail motion filled the testing arena.

For each trial, we placed 10 mosquitoes in the simulator. At the beginning of the trial, we shook the container, causing all mosquitoes to take flight. Each trial lasted for 2 min, and we performed experiments for a maximum of 1.5 h at a time, allowing the mosquitoes to rest with access to sugar water for at least 3 h before beginning experiments again. We conducted 51 trials total with the fan attachment, consisting of 17 different tip speeds and three repeats of each speed. We ran the fan at a constant speed between 0 and 8.75 Hz in increments of approximately 0.5 Hz, leading to fan tip speeds u of 0–5.6 m s⁻¹. We conducted 15 trials with the single blade attachment, consisting of five different tip speeds and three repeats of each speed. The frequencies of the single blade attachment varied between 0 and 7.5 Hz in increments of approximately 2 Hz, corresponding to tip speeds between 0 and 4.9 m s⁻¹.

We filmed mosquitoes moving in our simulator to understand how the moving tail influences their motion. Fig. 4 compares the flight trajectories of mosquitoes when the fan is stationary (Fig. 4A,B) and when the fan is moving at a speed of 380 cm s⁻¹ (6 Hz) (Fig. 4C,D). The initial location of the flying mosquito is marked by circles in the figure. The mosquitoes fly upwards, reaching a peak position as shown, and the final resting location of the mosquitoes is marked by the asterisks. When the fan was stationary, they flew up to a maximum height of $z=1.5\pm3.3$ cm below the fan and landed at an average height of $z=4.9\pm6.2$ cm below the fan ($N=17$). If the fan was moving, however, the mosquitoes flew to an average height of $z=1.6\pm2.1$ cm below the fan and then flew back down to a distance of $z=9.0\pm5.2$ cm below the fan ($N=17$). It appears the mosquitoes are not aware of the fan until they are sufficiently close, but then veer off and land farther away. The landing distance when the fan is on is nearly twice as far as that when the fan is stationary.

To determine how much air flow is created by the tail, we modeled the tail as Stokes' oscillating plate. Consider an infinite one-dimensional plate extending in the x direction. We consider the effects of in-plane oscillations at frequency f on the flow as a distance z from the plate. We consider the plate oscillating at a maximum speed, u_0, of 380 cm s⁻¹ with a frequency, f, of 6 Hz. Solving the Navier–Stokes equations (Panton, 2013) yields the

velocity profile of the air below the fan:

$$u(z,t) = u_0 \exp\left(-z\sqrt{\frac{2\pi f}{2v}}\right) \sin\left(2\pi ft - z\sqrt{\frac{2\pi f}{2v}}\right), \quad (14)$$

where v is the kinematic viscosity of air at room temperature, 1.46×10^{-5} m^2 s^{-1}. The air speed decays exponentially with distance. It is 380 cm s^{-1} at z=0 cm, 1.3 cm s^{-1} at z=0.5 cm and 0.004 cm s^{-1} at z=1 cm. Thus, at a distance z=0.5 cm below the fan, the mosquitoes still feel the effects of the fan. This critical distance explains why mosquitoes fly close to the fan before being repelled to a farther and more comfortable distance.

We then examined the fraction, p_i, of mosquitoes that land above the blades. Below, we use the notation p_f for the fan attachment, p_o for the oscillating single blade attachment and p_s for the ShooAway™. Fig. 3D–F shows the relationship between p_i and the tip speed u, where the linear best fit line is given by:

$$p_f = -8.0u + 37 \quad (R^2 = 0.73), \quad (15)$$

$$p_o = -3.5u + 21 \quad (R^2 = 0.73), \quad (16)$$

$$p_s = -6.8u + 63 \quad (R^2 = 1). \quad (17)$$

For both the single-blade attachment and the fan attachment, faster motions repelled more mosquitoes, but with diminishing returns. This can be seen by comparing Fig. 3D and 3E as well as Eqns 15 and 16. To understand how mammals choose the speed of their tails, we consider the speeds of mosquitoes and the animals in our study.

The average tail tip speeds for the animals measured in this study ranged from 0.85 m s^{-1} for an elephant to 6.31 m s^{-1} for a large dog. When comparing the tip speeds to the flight speed of mosquitoes, we only considered the horse, zebra and elephant because these animals swished their tails in response to insects during filming, whereas dogs responded to other things in their environment, such as the humans filming them. The blue rectangle below the x-axis in Fig. 3D represents the 0.85–1.17 range in tail tip speeds, which we call u_r, for the elephant, horse and zebra, including their standard deviations. When the fan spun at this range of speeds, it prevented 60 to 85% of mosquitoes from landing.

When the fan is off, not all of the mosquitoes land on the ceiling of the simulator. So, we define effectiveness of the simulator e_i as the fraction of mosquitoes repelled when the fan is off divided by the fraction of the mosquitoes repelled when the fan is spinning in the range u_r:

$$e_i = \frac{1 - p_i(u = 0)}{1 - p_i(u_r)}. \quad (18)$$

At u=0, 40% of the mosquitoes are repelled, leading to an effectiveness e_s of 50% for the steady-state motion.

Oscillatory motions seem to be even less effective: at the speeds of mammal tails, the oscillations prevented 82% of mosquitoes from landing, whereas when the oscillation is off, 80% are repelled. By Eqn 18, this means the oscillation was only 1% effective. The reason the oscillatory motion appears to be less effective than the steady-state motion is because so few mosquitoes landed on the top board when the motor was off. The vertical wall dividing the cylinder in the oscillatory experiments provides the mosquitoes a convenient place to land, so they did not continue flying upward as they did in the steady-state fan experiments. For that reason, we neglect results of the oscillatory tests and consider only the steady-state tests as

simulating the mammal tail. We thus conclude that mammals can repel up to 50% of the mosquitoes from landing, relative to the number that would land if the tail were stationary.

Mosquitoes fly at an average speed of approximately 0.3 m s^{-1} (Hoffmann and Miller, 2003) and a maximum speed of 1.4–1.8 m s^{-1} (Gillies and Wilkes, 1981). This region is represented by the green rectangle in Fig. 3D, which notably falls in the same regime as mammal tail speeds. Our experiments thus rationalize why animals swish their tails at such a high speed, to repel mosquitoes by generating wind speeds comparable to the mosquito's flight speed. Moving the tail at higher speeds would indeed reduce the influx of mosquitoes, but may not be biologically possible for the animals.

We note that mosquitoes were generally unable to fly past the fan when it moved at speeds of 4.5 m s^{-1}, a speed that is much higher than the mosquito flight speed. The few mosquitoes that flew past the fan in this case were likely taking advantage of artifacts in our apparatus, such as flying along the walls of the container where air speed is affected by boundary effects.

Using our measurements of the effect of air flow on mosquitoes, we can now comment on current devices that use such strategies to repel mosquitoes. The ShooAway™ varies its spinning frequency from 3 to 5 Hz, with corresponding tip speeds ranging from 4 to 6 m s^{-1}. To test the effectiveness of this device, the experiment was repeated using the ShooAway™ in place of the fan, as shown in Fig. 3C. The ShooAway™ prevented 70% of the mosquitoes from landing behind it, as shown in Fig. 3F. When the ShooAway™ is off, 37% of the mosquitoes are repelled, so using Eqn 18, we found that the ShooAway™ is 53% effective at repelling mosquitoes. This is within the range of effectiveness of the fan when it is moving at tip speeds comparable to the mammal tail tip speeds, making the ShooAway™ just as effective at repelling mosquitoes as a mammal tail. However, the ShooAway™ spins much faster than the mammal tails. We conclude that the speed of the device is far too high. Its average speed is five times faster than that of a mammal tail, meaning it uses 25 times more power. It would be just as effective if it rotated at a tip speed comparable to that at which mammals swish their tails.

At its average tip speed, the ShooAway™ is not nearly as effective as the fan, which repels nearly all the mosquitoes. This could be explained by the fact that the ShooAway™ varies its spinning speed. This variation in speed is likely giving the mosquitoes a greater chance to fly past the blades. It should also be noted that that the ShooAway™ blades are longer than the blades on the simulator and are flexible enough that they droop by gravity, leaving more space between them and the top of the container. This gap could give the mosquitoes more room to find their way to the top, which in turn could partially account for the greater number of mosquitoes that are able to fly past it.

The tail swat

What happens when an insect makes it through the wind barrier and lands on the animal? In this section, we analyze and compare the dynamics of tail swats. The elephant and giraffe have tail swatting motions that can easily be seen by filming directly behind the animal, as shown in Fig. 5B,E. We assume the tail of the elephant is 11 kg (Robertson-Bullock, 1962), and Zoo Atlanta staff Stephanie Braccini reports the giraffe tail mass as 3 kg.

We used differential equations to model the tail, as shown in the Materials and Methods. We idealized the tail as a double pendulum, consisting of two segments of lengths L_1 and L_2, corresponding to the base of the tail, the part that has bones, and the end part of the tail, the part that is only hair. A schematic of this model and its

corresponding sections on the real elephant tail are shown in Fig. 5A and the first frame of Fig. 5B, respectively. We tracked three points on the tail: the base of the tail (point 1 in Fig. 5A,B), the end of the bony part of the tail (point 2), and the end of the hairy part (point 3). Fig. 5C,F shows the time course of point B, where experiments are given by the closed symbols and the predictions of our mathematical model are shown by the solid line.

The only free parameter to this model is the input torque at the base of the tail. The values of the input torque for each animal are shown in Fig. 5D,G. Movie 3 shows the motion of the elephant's tail and our prediction. As shown by the movie and the experimental and predicted trajectories in Fig. 5C, overall, the model is successful at predicting the trajectories of both the initial swish of the tail and the swat in the elephant. The swish phase is shown by the first three periods in Fig. 5C. To generate these swings, our model applied a base torque of 15 N m for 1 s and then for the next 3.6 s the pendulum was allowed to swing freely with no additional torque.

We now consider how the elephant swats the insect. A swat consists of three phases: the preparatory swing (the first frame in Fig. 5B), the strike (frames 2 through 4) and the recovery swing (the last frame). During the preparatory swing, the elephant increases the amplitude of its swing. While a typical amplitude of the swish phase is 17 deg, the preparatory swing involves an amplitude of 40 deg. During the strike phase, the amplitude increases to 117 deg. The frequency of the tail also increases, but less so, increasing by 16% of the average swishing frequency. To create such a large motion, the base of the tail requires a torque of 350 N m. This torque is approximately the same torque produced by a Honda Accord sedan (https://automobiles.honda.com/accord-sedan#specifications). An elephant can produce a maximum torque of 2500 N m to move its leg (Biewener, 1989; Fuentes, 2016; Ren et al., 2010), so we surmise that a torque of 350 N m is well within the range of what an elephant can produce. Additionally, a torque of 200 N m is required for a 75 kg human to jump (Wensing et al., 2017).

When the pendulum reaches its maximum amplitude, a substantial counter-clockwise torque is required to slow it down. This braking is likely accomplished by the tendon and muscles of the tail. This makes sense when thinking of a softball batter's swing. After the batter has hit the ball and is following through on the swing, she must resist the motion of the bat to stop it and prevent it from flying out of her hands and over her shoulders. Likewise, the elephant must control its tail so that it can regroup quickly and prepare to swat again. The third and final stage of the swat involves a return to a normal swishing amplitude and frequency in the recovery swing.

Giraffes differ from the other animals in this study in that they do not constantly exhibit the swishing behavior, maybe because of the long length of the tail, 0.9 m. Rather, they will swat their tails from a standstill, presumably when they feel an insect land on them. The tail reaches a maximum amplitude of 85 deg with a torque of 40 N m over 0.2 s. Such torque values are feasible: a torque of 40 N m is required to swing a human leg at 1.1 Hz (Doke et al., 2005), and an average woman's leg weighs 3.3 kg (Plagenhoef et al., 1983), similar to the giraffe tail. The giraffe swat actually decreases in frequency by 71% from the average swishing frequency. This is the reverse of the change in frequency measured in the elephant swat, and could be due to the differences in the general tail swishing behaviors of the two animals.

The elephant took 1.3 s and the giraffe took 0.63 s to complete the swat, starting from the beginning of the preparatory swing to the time when the tail reached its greatest amplitude in the strike phase. This time scale is on the same order as that required to swat an insect

before it bites. A fly will take off 200 ms after seeing an incoming object (Card and Dickinson, 2008), and biting insects spend only a few seconds biting and searching for a blood vessel (Choumet et al., 2012; Chappuis et al., 2013). Clearly, speed is important to mammals attempting to defend themselves from biting insects.

DISCUSSION

While it is widely observed that mammals use their tails to defend against insects, little is understood of the mechanism. We have shown that the tail affords two means of defense: wind generation and high-speed swatting. During the high-frequency swishing phase, the tail creates an air flow sufficiently high enough to blow insects away from the body of the animal. Our results here agree with those of previous studies of mosquitoes flying in the wind, which show that wind negatively affects (1) a mosquito's ability to detect and land on a host (Hoffmann and Miller, 2002; Service, 1980), and (2) the number of mosquitoes caught in traps (Hoffmann and Miller, 2003; Bidlingmayer et al., 1995).

We have shown the tail to be effective at repelling mosquitoes, but it may be less effective with faster insects. Whereas small insects such as mosquitoes are limited to 1 m s^{-1} flight speeds (Dudley, 2002), larger insects can fly much faster, with one study finding that insects fly at speeds from 0.4 to 8 m s^{-1} (Dudley, 2002). As the speed of the insect increases, the effectiveness of the tail likely diminishes. However, a mammal's many other defensive behaviors, such as muscle twitching, head shaking and ear twitching, likely aid in protecting them from fast insects. Additionally, most mammal tails are black or dark in color, so visual cues could also help deter flying insects (Horváth et al., 2010). The speed of the insect should not alter the effectiveness of the tail swat, which acts when insects are stationary.

Tail swishing frequency decreases with increasing body size, which is consistent with other observations of reciprocal motion in animals. Froude's law states that body speed should scale with body length to the 1/2 power (McMahon and Bonner, 1983). Using Eqns 5 and 6 and assuming amplitude is a constant, Froude's law gives $f{\sim}M^{-0.12}$, which is similar to the scaling we found of $f{\sim}M^{-0.19}$. Mammals remove water from their bodies by shaking at a frequency of $f{\sim}M^{-0.22}$ (Dickerson et al., 2012). Stride frequency at the transition from trot to gallop in mammals scales as $f{\sim}M^{-0.15}$, and the frequencies at the trot and gallop are $f{\sim}M^{-0.13}$ and $f{\sim}M^{-0.16}$, respectively (Heglund and Taylor, 1988). Wing beat frequencies scale as $f{\sim}M^{-0.26}$ in bats and $f{\sim}M^{-0.27}$ in birds (Norberg and Norberg, 2012).

The swatting motion is an example of an animal applying forces only at the base of a flexible appendage yet still being very precise with its endpoint. Although there are muscles throughout the tail, our simulation suggests that the muscles do not need to be active to score a precise hit. Swinging up a pendulum is a classic optimization and controls problem that has long been of interest to roboticists (Åström and Furuta, 2000). Understanding how mammals control their own tails could lead to solutions for legged robots (Hubicki et al., 2016; Birn-Jeffery et al., 2014).

Our results expand our understanding of the use of tails in mammals, and can help us understand how altering their tails can affect the well-being of an animal. For example, tail docking is a procedure by which the distal tail vertebrae are amputated. It occurs in large numbers of horses for aesthetic reasons, but recently this practice has been challenged because it causes unnecessary pain and health risks to the animals (Lefebvre et al., 2007). Although there are arguments (Lefebvre et al., 2007) that docking improves a horse's hygiene and welfare, the results of our study suggest that

shortening the tail length would inhibit a horse's ability to shoo away hazardous biting insects.

In this study, we elucidated how mammals use their tails to repel insects. We showed through experiments that mammals swish their tails at the speed of a flying mosquito, presenting a physical as well as a wind barrier to prevent insects from landing. When mosquitoes land, they can swat at them at a high speed before they have a chance to bite. The trajectory of the swat is well predicted by modeling it as a double pendulum and controlling the input torque only at the base. Mosquitoes are responsible for the death of several million people each year (World Health Organization, 1996), and the results presented in this study could be used to create a low-energy device that creates a small air flow and repels mosquitoes away from people.

Supplementary information
Supplementary information available online at
http://jeb.biologists.org/lookup/doi/10.1242/jeb.178905.supplemental

References
Åström, K. J. and Furuta, K. (2000). Swinging up a pendulum by energy control. *Automatica* **36**, 287-295.

Beer, R. (2003). *The Handbook of Tibetan Buddhist Symbols*. Chicago, IL: Serindia Publications, Inc.

Bidlingmayer, W., Day, J. and Evans, D. (1995). Effect of wind velocity on suction trap catches of some Florida mosquitoes. *J. Am. Mosq. Control Assoc.* **11**, 295-301.

Biewener, A. A. (1989). Mammalian terrestrial locomotion and size. *Bioscience* **39**, 776-783.

Birn-Jeffery, A. V., Hubicki, C. M., Blum, Y., Renjewski, D., Hurst, J. W. and Daley, M. A. (2014). Don't break a leg: running birds from quail to ostrich prioritise leg safety and economy on uneven terrain. *J. Exp. Biol.* **217**, 3786-3796.

Card, G. and Dickinson, M. H. (2008). Visually mediated motor planning in the escape response of *Drosophila*. *Curr. Biol.* **18**, 1300-1307.

Chappuis, C. J. F., Béguin, S., Vlimant, M. and Guerin, P. M. (2013). Water vapour and heat combine to elicit biting and biting persistence in tsetse. *Parasit. Vectors* **6**, 240.

Choumet, V., Attout, T., Chartier, L., Khun, H., Sautereau, J., Robbe-Vincent, A., Brey, P., Huerre, M. and Bain, O. (2012). Visualizing non infectious and infectious *Anopheles gambiae* blood feedings in naive and saliva-immunized mice. *PLoS ONE* **7**, e50464.

Cowell, D. D., Hall, M. J. and Scholl, P. J. (2006). *The Oestrid Flies: Biology, Host–Parasite Relationships, Impact and Management*. Wallingford: CAB International.

Dickerson, A. K., Mills, Z. G. and Hu, D. L. (2012). Wet mammals shake at tuned frequencies to dry. *J. R Soc. Interface* **9**, 3208-3218.

Doke, J., Donelan, J. M. and Kuo, A. D. (2005). Mechanics and energetics of swinging the human leg. *J. Exp. Biol.* **208**, 439-445.

Dudley, R. (2002). *The Biomechanics of Insect Flight: Form, Function, Evolution*. Princeton, NJ: Princeton University Press.

Dudley, R. and Milton, K. (1990). Parasite deterrence and the energetic costs of slapping in howler monkeys, *Alouatta palliata*. *J. Mammal.* **71**, 463-465.

Edman, J. D. and Scott, T. W. (1987). Host defensive behaviour and the feeding success of mosquitoes. *Int. J. Trop. Insect Sci.* **8**, 617-622.

Foil, L. and Foil, C. (1988). Dipteran parasites of horses. *Equine Practice* **10**, 21-38.

Fuentes, M. A. (2016). Theoretical considerations on maximum running speeds for large and small animals. *J. Theor. Biol.* **390**, 127-135.

Gillies, M. T. (1955). The density of adult anopheles in the neighbourhood of an east African village. *Am. J. Trop. Med. Hyg.* **4**, 1103-1113.

Gillies, M. T. and Wilkes, T. J. (1981). Field experiments with a wind tunnel on the flight speed of some West African mosquitoes (Diptera: Culicidae). *Bull. Entomol. Res.* **71**, 65-70.

Greenwood, D. T. (2003). *Advanced Dynamics*. New York: Cambridge University Press.

Hart, B. L. (1990). Behavioral adaptations to pathogens and parasites: five strategies. *Neurosci. Biobehav. Rev.* **14**, 273-294.

Harvey, T. L. and Launchbaugh, J. L. (1982). Effect of horn flies on behavior of cattle. *J. Econ. Entomol.* **75**, 25-27.

Heglund, N. C. and Taylor, C. R. (1988). Speed, stride frequency and energy cost per stride: how do they change with body size and gait? *J. Exp. Biol.* **138**, 301-318.

Hickman, G. C. (1979). The mammalian tail: a review of functions. *Mammal. Rev.* **9**, 143-157.

Hoffmann, E. J. and Miller, J. R. (2002). Reduction of mosquito (Diptera: Culicidae) attacks on a human subject by combination of wind and vapor-phase deet repellent. *J. Med. Entomol.* **39**, 935-938.

Hoffmann, E. J. and Miller, J. R. (2003). Reassessment of the role and utility of wind in suppression of mosquito (Diptera: Culicidae) host finding: stimulus dilution supported over flight limitation. *J. Med. Entomol.* **40**, 607-614.

Horváth, G., Blahó, M., Kriska, G., Hegedüs, R., Gerics, B., Farkas, R. and Åkesson, S. (2010). An unexpected advantage of whiteness in horses: the most horsefly-proof horse has a depolarizing white coat. *Proc. R. Soc. B* **277**, 1643-1650.

Hubicki, C., Grimes, J., Jones, M., Renjewski, D., Spröwitz, A., Abate, A. and Hurst, J. (2016). Atrias: design and validation of a tether-free 3D-capable spring-mass bipedal robot. *Int. J. Robotics Res.* **35**, 1497-1521.

Keiper, R. R. and Berger, J. (1982). Refuge-seeking and pest avoidance by feral horses in desert and island environments. *Appl. Anim. Ethol.* **9**, 111-120.

Lefebvre, D., Lips, D., Ödberg, F. O. and Giffroy, J. M. (2007). Tail docking in horses: a review of the issues. *Animal* **1**, 1167-1178.

McMahon, T. A. (1975). Using body size to understand the structural design of animals: quadrupedal locomotion. *J. Appl. Physiol.* **39**, 619-627.

McMahon, T. A. and Bonner, J. T. (1983). *On Size and Life*. New York: Scientific American Library.

Moore, J. (2002). *Parasites and the Behavior of Animals. Oxford Series in Ecology and Evolution*. Oxford: Oxford University Press.

Mooring, M. S. and Hart, B. L. (1992). Animal grouping for protection from parasites: selfish herd and encounter-dilution effects. *Behaviour* **123**, 173-193.

Mooring, M. S., Blumstein, D. T., Reisig, D. D., Osborne, E. R. and Niemeyer, J. M. (2007). Insect-repelling behaviour in bovids: role of mass, tail length, and group size. *Biol. J. Linn. Soc.* **91**, 383-392.

Norberg, U. M. L. and Norberg, R. Å. (2012). Scaling of wingbeat frequency with body mass in bats and limits to maximum bat size. *J. Exp. Biol.* **215**, 711-722.

Nowak, R. M. (1999). *Walker's Mammals of the World*, Vol. 2, 6th edn. Baltimore, MD: Johns Hopkins University Press.

Panton, R. L. (2013). *Incompressible Flow*, 4th edn. Hoboken, NJ: John Wiley and Sons.

Plagenhoef, S., Evans, F. G. and Abdelnour, T. (1983). Anatomical data for analyzing human motion. *Res. Q Exerc. Sport* **54**, 169-178.

Ren, L., Miller, C. E., Lair, R. and Hutchinson, J. R. (2010). Integration of biomechanical compliance, leverage, and power in elephant limbs. *Proc. Natl Acad. Sci. USA* **107**, 7078-7082.

Riegel, G. T. (1979). The fly whisk. *Bull. Entomol. Soc. Am.* **25**, 196-199.

Robertson-Bullock, W. (1962). The weight of the African elephant *Loxodonta africana*. *J. Zool.* **138**, 133-135.

Rogan, E. L. (2012). *The Arabs: A History*. New York: Basic Books.

Samuel, W. M., Pybus, M. J. and Kocan, A. A. (2001). *Parasitic Diseases of Wild Mammals*, 2nd edn. Ames, IA: Iowa State University Press.

Service, M. W. (1980). Effects of wind on the behaviour and distribution of mosquitoes and blackflies. *Int. J. Biometeorol.* **24**, 347-353.

Siegfried, W. R. (1990). Tail length and biting insects of ungulates. *J. Mammal.* **71**, 75-78.

Tashiro, H. and Schwardt, H. H. (1953). Biological studies of horse flies in New York. *J. Econ. Entomol.* **46**, 813-822.

Taylor, D. B., Moon, R. D. and Mark, D. R. (2012). Economic impact of stable flies (Diptera: Muscidae) on dairy and beef cattle production. *J. Med. Entomol.* **49**, 198-209.

Toupin, B., Huot, J. and Manseau, M. (1996). Effect of insect harassment on the behaviour of the Rivière George caribou. *Arctic* **49**, 375-382.

Waage, J. and Nondo, J. (1982). Host behaviour and mosquito feeding success: an experimental study. *Trans. R. Soc. Trop. Med. Hyg.* **76**, 119-122.

Walker, J. (2007). *The Flying Circus of Physics*, 2nd edn. Hoboken, NJ: John Wiley and Sons.

Warnes, M. L. and Finlayson, L. H. (1987). Effect of host behaviour on host preference in *Stomoxys calcitrans*. *Med. Vet. Entomol.* **1**, 53-57.

Wensing, P. M., Wang, A., Seok, S., Otten, D., Lang, J. and Kim, S. (2017). Proprioceptive actuator design in the mit cheetah: impact mitigation and high-bandwidth physical interaction for dynamic legged robots. *IEEE Trans. Robot.* **33**, 509-522.

Williams, C. A. S. (2006). *Chinese Symbolism and Art Motifs: A Comprehensive Handbook on Symbolism in Chinese Art through the Ages*, 2nd edn. New York: Tuttle Publishing.

World Health Organization (1996). *The world health report 1996 – fighting disease, fostering development*. Technical report. Geneva: World Health Organization.